Elastic-constant anomalies in $YbPO_4$

J. Nipko
Argonne National Laboratory, Argonne, Illinois 60439
and Colorado State University, Fort Collins, Colorado 80523

M. Grimsditch and C.-K. Loong
Argonne National Laboratory, Argonne, Illinois 60439

S. Kern
Colorado State University, Fort Collins, Colorado 80523

M. M. Abraham and L. A. Boatner
Oak Ridge National Laboratory, Oak Ridge, Tennessee 37831
(Received 27 April 1995)

The elastic constants of $YbPO_4$ have been determined in the temperature range from 10 to 300 K by using Brillouin scattering techniques. An approximate 20% softening of the $\frac{1}{2}(C_{11}-C_{12})$ elastic constant was observed, and this anomaly suggests that a Jahn-Teller-type coupling occurs between the low-lying electronic states of the Yb^{3+} ions and the B_{1g} lattice strain mode even though a cooperative structural phase transition does not take place.

INTRODUCTION

Interactions between rare-earth (R) ions and the host lattice in rare-earth orthophosphates and orthovanadates have provided the motivation for a number of spectroscopic studies during the past two decades.[1–4] Orthophosphate and orthovanadate systems are ideal candidates for carrying out systematic investigations for two important reasons: first, the orthophosphates, RPO_4 (R=Tb to Lu), and the orthovanadates, RVO_4 (R=Ce to Lu), have a relatively simple body-centered tetragonal-crystal structure of the zircon type (space group $I4_1/amd$) in which the R ions occupy sites of unique point-group symmetry D_{2d}; second, in these tetragonal-symmetry insulating materials, rare-earth crystal-field transitions and phonons represent the primary excitations that are responsible for the spin-lattice coupling. In general, coupling of the rare-earth and lattice subsystems may lead to anomalous elastic behavior and/or vibronic excitations/relaxations. In the extreme case, a cooperative Jahn-Teller phase transition occurs, resulting in a distortion of the tetragonal lattice to a lower symmetry—accompanied by a renormalization of the rare-earth electronic states. The degree of such anomalies, if present, depends to a large extent on the compatibility of the rare-earth ground and low-lying state wave functions with respect to the lattice strain fields and phonon symmetries.[2–4] In order to characterize the R level structure and the phonon states, we have initiated a systematic study[5–9] of the RPO_4 compounds by neutron crystal-field spectroscopy and lattice dynamics measurements. The present work reports the observation of an anomalous softening of the $\frac{1}{2}(C_{11}-C_{12})$ elastic constant in $YbPO_4$ at low temperatures as observed by Brillouin scattering methods.

Among the tetragonal RPO_4 compounds (R from Tb to Lu), only $TbPO_4$ exhibits a cooperative Jahn-Teller phase transition which takes place at about 2.2 K. The third-order magnetic susceptibility and parastriction data for $TbPO_4$ have recently been analyzed by Morin and co-workers[10] using a susceptibility formalism. In the case of $TmPO_4$, Harley and Manning[11] reported a softening of the C_{66} elastic constant with decreasing temperature based on measurements made using an ultrasonic technique. The C_{66} value reaches a nonzero minimum at about 20 K followed by an increase at lower temperatures. These authors interpreted the data by employing a model developed previously by Elliott and co-workers[1] and by Sandercock and co-workers[12] for the analysis of the Jahn-Teller effects in $TbVO_4$ and $DyVO_4$. Although this model only considers the coupling of a subset of relevant crystal-field states to certain lattice strain fields and/or phonon modes, it permits a useful analysis of the elastic-constant anomalies in terms of a few Jahn-Teller-interaction parameters. In the present study of $YbPO_4$, we have observed an overall $\sim$20% softening of the $\frac{1}{2}(C_{11}-C_{12})$ elastic constant in the temperature range between 300 and 15 K. This result indicates an underlying tendency of the $YbPO_4$ lattice to undergo an orthorhombic distortion along the a and b axes via a coupling to the B_{1g} strain as opposed to coupling to the B_{2g} strain in $TmPO_4$.

In this work, we present the elastic constants of $YbPO_4$ measured by Brillouin-scattering techniques. All of the room temperature elastic constants (with the exception of C_{13}), as well as the temperature dependence of the C_{11}, C_{44}, C_{66}, $\frac{1}{2}(C_{11}-C_{12})$ and $\frac{1}{2}(C_{11}+C_{12}+2C_{66})$ for $YbPO_4$ are given. The results for the C_{11} and C_{66} elastic constants are compared to those obtained for the nonmagnetic compound $LuPO_4$.

EXPERIMENT

Single crystals of $YbPO_4$ and $LuPO_4$ were grown using a flux technique described previously.[13] The elastic properties

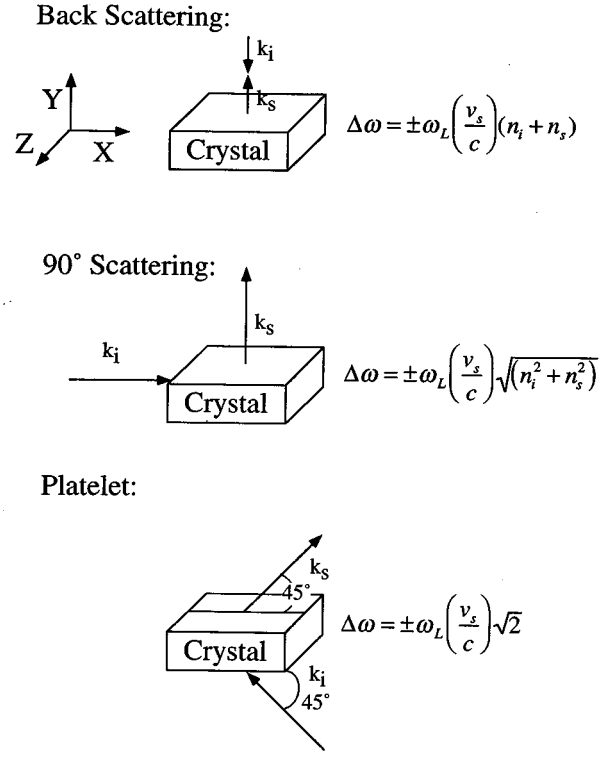

FIG. 1. Schematic diagram of the scattering geometries and corresponding frequency shifts expressed in terms of the incident laser frequency (ω_L), speed of light in vacuum (c), sound velocity (v_s), and the indices of refraction for the incident and scattered radiation (n_i and n_s).

of $YbPO_4$ and $LuPO_4$ were measured using the technique of Brillouin scattering. Since thorough reviews[14–16] of the Brillouin-scattering technique can be found in the literature, we will restrict the current discussion only to the aspects necessary for interpreting our experimental results.

An argon laser operating at a power of 300 mW and a wavelength of 5145 Å was used, and the single-crystal samples (typical dimensions $1\times1\times7$ mm^3) were cooled using a Heli-Trans cryostat for measurements over a temperature range of 10–300 K. The three scattering geometries used for the room-temperature measurements are depicted in Fig. 1. Only the back-scattering and 90°-scattering geometries were used for the temperature dependence measurements. Most of the measurements were carried out using a 5+4 pass tandem Fabry-Pérot interferometer.[16] However, in the 90°-scattering geometry, it was necessary to compensate for the decrease of Brillouin intensity with decreasing temperature by operating in 5 pass without the tandem etalon for low-temperature measurements.

RESULTS AND DISCUSSION

Brillouin scattering can be viewed as inelastic scattering of light from fluctuations produced by long-wavelength acoustic waves. The frequency shift of a Brillouin line is given by[17]

$$\Delta\omega = \pm\omega_L\left(\frac{v_s}{c}\right)(n_i^2 + n_s^2 - 2n_i n_s\cos\theta)^{1/2}, \qquad (1)$$

TABLE I. Roots of the Christoffel equation for elastic waves of polarization **u** and wave vector **q** (l and n are the direction cosines; L and T denote longitudinal and transverse; QL and QT indicate quasilongitudinal and quasitransverse).

q	**u**	ρv_s^2
(1,0,0)	(1,0,0):L	C_{11}
	(0,1,0):T	C_{66}
	(0,0,1):T	C_{44}
$\left(\frac{1}{\sqrt2},\frac{1}{\sqrt2},0\right)$	$\left(\frac{1}{\sqrt2},\frac{1}{\sqrt2},0\right)$:$L$	$\frac{1}{2}(C_{11}+C_{12}+2C_{66})$
	$\left(\frac{1}{\sqrt2},-\frac{1}{\sqrt2},0\right)$:$T$	$\frac{1}{2}(C_{11}-C_{12})$
	(0,0,1):T	C_{44}
(l,0,n)	(l,0,n):QL	$\frac{1}{2}(R_1+\sqrt{R_2})$
	(n,0,$-l$):QT	$\frac{1}{2}(R_1-\sqrt{R_2})$
	(0,1,0):T	$n^2C_{44}+l^2C_{66}$

$R_1 = l^2C_{11} + C_{44} + n^2C_{33}$

$R_2 = (l^2C_{11} - n^2C_{33})[l^2C_{11} - n^2C_{33} - 2C_{44}(l^2 - n^2)] + C_{44}^2 + 4n^2l^2C_{13}(C_{13} + C_{44})$

where ω_L is the laser frequency, v_s is the sound velocity, c the speed of light in vacuum, θ the scattering angle (inside the crystal), and n_i and n_s indices of refraction for the incident and scattering radiation, respectively. The frequency shifts for the scattering geometries used are given in Fig. 1.

For using Eq. (1) (or the simplified expressions given in Fig. 1) to extract sound velocities from measured frequency shifts the following sources of error must be considered: uncertainties in the scattering angle and the refractive indices, and error in determining the position of the Brillouin peaks. The latter are random errors and lead to the observed spread in the experimental data. Uncertainties in scattering angle and the indices of refraction produce vastly different effects depending on which scattering geometry is being used. For example, in the back-scattering geometry, errors in scattering angle are typically negligible; in the platelet geometry uncertainties in the indices of refraction are unimportant.

In order to assign measured velocities to specific elastic constants it is necessary to know the crystallographic orientation of the sample relative to the scattering geometry. The particular combination of elastic constants which determines the sound velocity for propagation along a given direction is obtained by solving the Christoffel equations. In Table I we have listed the combination of elastic constants for the propagation directions studied in this investigation.

The refractive indices of $YbPO_4$ have not yet been reported; therefore, they have been determined by combining results from the various scattering geometries. Our room-temperature results are summarized in Table II; the quoted errors are based on estimates of the uncertainty in the scattering angle and the uncertainty in determining the positions of the Brillouin-peak maxima. Also shown in Table II are the C_{ij} for $LuPO_4$ that was obtained previously by Armbruster and co-workers.[18]

In Fig. 2, the temperature dependence of the elastic con-

TABLE II. Room-temperature elastic constants, indices of refraction, and density (C_{ij} in 10^{12} dyn/cm^2).

$LuPO_4$[a]	$YbPO_4$[b]
$C_{11}=3.20\pm0.03$	$C_{11}=2.92\pm0.03$
$C_{12}=0.36\pm0.07$	$C_{12}=0.22\pm0.05$
$C_{13}=1.15\pm0.5$	$C_{13}=$(not obtained)
$C_{33}=3.82\pm0.14$	$C_{33}=3.15\pm0.07$
$C_{44}=0.846\pm0.008$	$C_{44}=0.87\pm0.02$
$C_{66}=0.217\pm0.002$	$C_{66}=0.35\pm0.02$
$n_0=1.694\pm0.005$	$n_0=1.72\pm0.01$
$n_e=1.728\pm0.005$	$n_e=1.81\pm0.01$
$\rho=6.508$ g/cm^3	$\rho=6.436$ g/cm^3

[a]Reference 17.
[b]This work.

stants C_{11} and C_{66} is presented for both $YbPO_4$ and $LuPO_4$. Lu^{3+} has a completely filled $4f$ shell and, therefore, in $LuPO_4$ no interactions between the phonon and electron systems are expected. We find that the C_{66} shows little dependence on temperature in both the Lu^{3+} and Yb^{3+} systems. However, the C_{11} of $YbPO_4$ softens by about 10% of the room-temperature value before leveling off at temperatures of about 30 K, while the C_{11} of $LuPO_4$ shows a slight stiffening of about 2%. In Fig. 3(a), the temperature dependence of the C_{44} and the combination $\frac{1}{2}(C_{11}+C_{12}+2C_{66})$ is given for $YbPO_4$ where we observed a slight stiffening of about

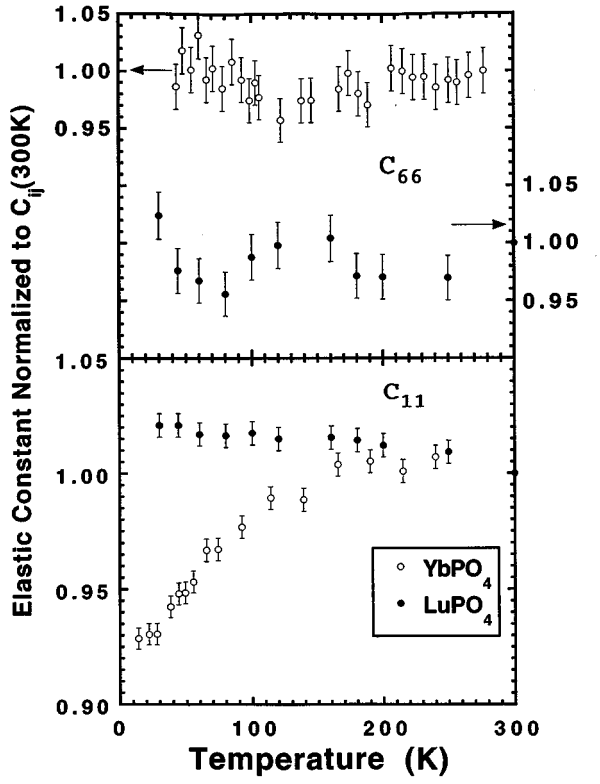

FIG. 2. Temperature dependence of C_{66} and C_{11} of $YbPO_4$ (○) and $LuPO_4$ (●). Data were taken in the back-scattering geometry.

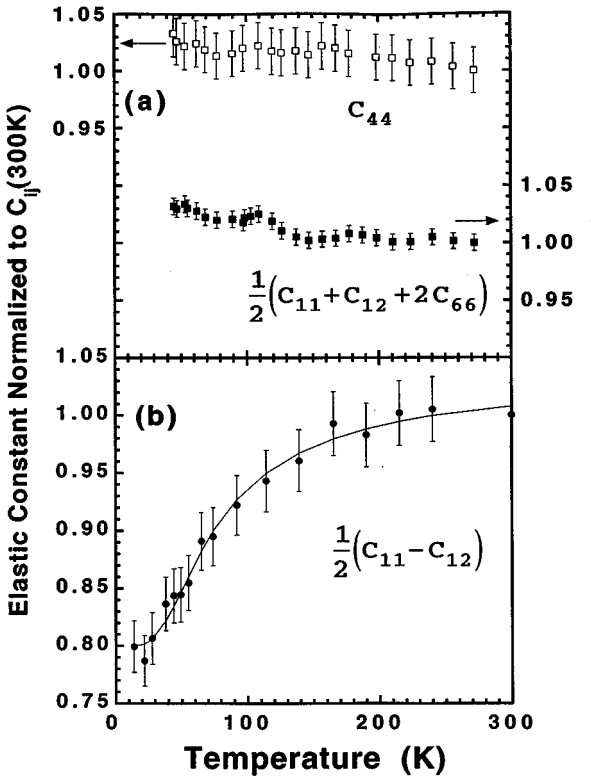

FIG. 3. (a) C_{44} and $\frac{1}{2}(C_{11}+C_{12}+2C_{66})$ for $YbPO_4$ normalized to their values at 300 K. Data were taken in the 90°-scattering geometry. (b) $\frac{1}{2}(C_{11}-C_{12})$ elastic constant for $YbPO_4$ normalized to its value at 300 K. The line is a fit using the model of mean-field theory (see text).

3.5% in both modes. Finally, Fig. 3(b) displays the temperature dependence of $\frac{1}{2}(C_{11}-C_{12})$ for $YbPO_4$. This graph was derived from a combined analysis of the 90°- and back-scattering data. Here, we see the $\frac{1}{2}(C_{11}-C_{12})$ mode softens by about 20%. The line through the data points represents a fit using the mean-field-theory model as given by Elliott and co-workers.[1] Specifically, the expression for the temperature dependence obtained from this model is

$$\tfrac{1}{2}(C_{11}-C_{12})(T)=\tfrac{1}{2}(C_{11}^0-C_{12}^0)\left[\frac{\varepsilon-J'\tanh\left(\frac{\varepsilon}{k_BT}\right)}{\varepsilon-J(0)\tanh\left(\frac{\varepsilon}{k_BT}\right)}\right], \tag{2}$$

where $\frac{1}{2}(C_{11}^0-C_{12}^0)$ is the elastic constant in the absence of ion-lattice interactions, $J(0)$ is the mean-field exchange-interaction parameter, $J'=J(0)+\eta$ is the mean-field parameter with an additional contribution due to the static strain, and 2ε is the crystal-field splitting between the ground and first excited states. Using $2\varepsilon=99.0$ cm^{-1}, obtained from a neutron-magnetic-scattering experiment as described below, a fit to Eq. (2) yields $\frac{1}{2}(C_{11}^0-C_{12}^0)=1.40\pm0.01\times10^{12}$ dyn/cm^2; $\eta=10.4\pm1.0$ cm^{-1}; and $J(0)=53.6\pm6.0$ cm^{-1}.

According to the Jahn-Teller theorem, four types of distortions corresponding to A_{1g}, B_{1g}, B_{2g}, and E_g symmetry are compatible with coupling of the R^{3+} electronic states in the tetragonal RPO_4 system. The A_{1g} mode does not change

the symmetry of the system and would produce only a uniform energy shift of the electronic states. Coupling to the doubly degenerate E_g mode, which induces a monoclinic distortion, would affect the temperature dependence of C_{44}. The B_{2g} mode induces an orthorhombic distortion along a direction bisecting the *a* and *b* axes in the basal plane. The coupling of electronic states to this mode would manifest itself as a temperature dependence of C_{66}. The B_{1g} mode induces an orthorhombic distortion along the *a* and *b* axes, coupling to this mode is revealed by the temperature dependence of the $\frac{1}{2}(C_{11}-C_{12})$ elastic constant.

From the above discussion, the present experimental results suggest that at low temperatures the $YbPO_4$ system tends to become unstable with respect to an orthorhombic distortion along the *a* and *b* axes, while couplings to the other modes are weak. The crystal-field level structure of Yb^{3+} ions in $YbPO_4$ was investigated by magnetic neutron spectroscopy at the Intense Pulsed Neutron Source (IPNS) of Argonne National Laboratory. The experimental procedure and data-analysis methods are similar to those described[9] for $HoVO_4$. Figure 4(a) displays the observed and calculated excitation spectrum where all the four Kramers doublets of the Yb^{3+} ground multiplet $^2F_{7/2}$ were identified. The peak at zero energy includes both elastic nuclear (Bragg) and magnetic scattering. A crystal-field model provides a fair representation of the energies and symmetry of the Yb wave functions, although the observed linewidths are much larger than those expected for a noninteracting single-ion system. Furthermore, the discrepancy in the observed and calculated intensity of the upper Γ_6 and Γ_7 states is due to strong electron-phonon coupling, as also revealed in the electronic Raman spectra obtained by Becker and co-workers.[19] Therefore, neutron and Raman data provide additional evidence for coupling of the Yb electronic states with phonons.

The interaction between the B_{1g} strain field and the electronic system can be qualitatively understood from the charge anisotropy of the two low-lying doublets of the Yb^{3+} ions. The ground state and the first-excited state at $\sim$12 meV ($\sim$140 K) contain a large $|\frac{7}{2},\pm\frac{3}{2}\rangle$ and $|\frac{7}{2},\pm\frac{1}{2}\rangle$ component, respectively, as shown in Fig. 4(b). The increased population of these states at low temperatures leads to a large quadrupole-moment component and an ''easy magnetization'' in the basal plane. From Fig. 4(b) it can be seen that the Γ_7 has a larger in-plane $4f$-charge density than the ground state Γ_6. Therefore, it is conceivable that a coupling of these anisotropic electronic states with lattice strains upon cooling may induce an instability toward an orthorhombic distortion starting at about 200 K. Below $\sim$30 K only the ground state is populated, the lesser anisotropy of the Γ_6 state will reduce the strength of electron-strain coupling, as evidenced by the saturated softening and the absence of a Jahn-Teller phase transition. The anomaly in the $\frac{1}{2}(C_{11}-C_{12})$ elastic constant from the present Brillouin-scattering study, in conjunction with the strong temperature-dependent mode mixing of two upper crystal-field transitions with an E_g optic phonon from neutron- and Raman-scattering[19] studies, indicate that $YbPO_4$ represents an important candidate for a detailed investigation of spin-lattice interaction in the RPO_4 systems.

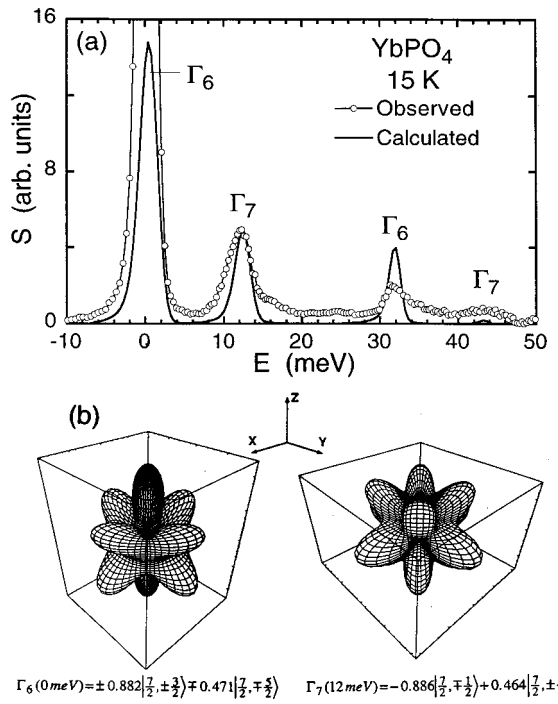

FIG. 4. (a) The observed neutron excitation spectrum of $YbPO_4$ as compared with calculation based on a noninteracting single-ion crystal-field model. The peak at zero energy is dominated by nuclear elastic scattering. The calculated spectrum was normalized to the observed peak intensity of the first Γ_7 state at 12 meV. (b) The spatial $4f$-charge distribution [defined according to Eq. (13) of Ref. 20] of the first two Yb crystal-field states from the model. The quantization axis (*z* direction) coincides with the crystallographic *c* axis of the $YbPO_4$ structure.

ACKNOWLEDGMENTS

We thank D. Renusch and S. Skanthakumar for their assistance in the data collection. Work performed at Argonne and Oak Ridge is supported by the U.S. DOE–BES under Contracts No. W-31-109-ENG-38 and No. DE-AC05-84OR21400, respectively.

[1] R. J. Elliott, R. T. Harley, W. Hayes, and S. R. P. Smith, Proc. R. Soc. London Ser. A **328**, 217 (1972).

[2] G. A. Gehring and K. A. Gehring, Rep. Prog. Phys. **38**, 1 (1975).

[3] R. L. Melcher, in *Physical Acoustics, Vol. 12*, edited by W. P. Mason and R. N. Thurston (Academic, New York, 1976), p. 1.

[4] R. T. Harley, in *Spectroscopy of Solids Containing Rare Earth Ions*, edited by A. A. Kaplyanskii and R. M. Macfarlane (Elsevier, The Netherlands, 1987), p. 557.

[5] C.-K. Loong, L. Soderholm, M. M. Abraham, L. A. Boatner, and N. M. Edelstein, J. Chem. Phys. **98**, 4214 (1993).

[6] C.-K. Loong, L. Soderholm, J. P. Hammonds, M. M. Abraham, L. A. Boatner, and N. M. Edelstein, J. Phys. Condens. Matter **5**, 5121 (1993).

[7] C.-K. Loong, L. Soderholm, G. L. Goodman, M. M. Abraham,

and L. A. Boatner, Phys. Rev. B **48**, 6124 (1993).
[8] S. Skanthakumar, C.-K. Loong, L. Soderholm, J. Nipko, J. W. Richardson, Jr., M. M. Abraham, and L. A. Boatner, J. Alloys Comp. **225**, 595 (1995).
[9] S. Skanthakumar, C.-K. Loong, L. Soderholm, M. M. Abraham, and L. A. Boatner, Phys. Rev. B **51**, 12 451 (1995).
[10] P. Morin, J. Rouchy, and Z. Kazei, Phys. Rev. B **50**, 12 625 (1994).
[11] R. T. Harley and D. I. Manning, J. Phys. C **11**, L633 (1978).
[12] J. R. Sandercock, S. B. Palmer, R. J. Elliott, W. Hayes, S. R. P. Smith, and A. P. Young, J. Phys. C **5**, 3126 (1972).
[13] M. Rappaz, L. A. Boatner, and M. M. Abraham, J. Chem. Phys. **73**, 1095 (1980).
[14] G. B. Benedek and K. Fritsch, Phys. Rev. **149**, 647 (1966).
[15] R. Vacher and L. Boyer, Phys. Rev. B **6**, 639 (1972).
[16] J. R. Sandercock, in *Light Scattering in Solids III*, edited by M. Cardona and G. Güntherodt, Topics in Applied Physics Vol. 51 (Springer, New York, 1978).
[17] M. H. Grimsditch and A. K. Ramdas, Phys. Rev. B **14**, 1670 (1976).
[18] A. Armbruster, R. Thomä, and H. Wehrle, Phys. Status Solidi *A* **24**, K71 (1974).
[19] P. C. Becker, G. M. Williams, N. M. Edelstein, J. A. Koningstein, L. A. Boatner, and M. M. Abraham, Phys. Rev. B **45**, 5027 (1992).
[20] U. Walter, Z. Phys. B **62**, 299 (1986).